

# Elevated Mercury Concentrations and Isotope Signatures (N, C, Hg) in Yellowfin Tuna (*Thunnus albacares*) from the Galápagos Marine Reserve and Waters off Ecuador

Laia Muñoz-Abril,<sup>a,b,c,\*</sup> Carlos A. Valle,<sup>a,b</sup> Juan José Alava,<sup>d</sup> Sarah E. Janssen,<sup>e</sup> Elsie M. Sunderland,<sup>f</sup> Francisco Rubianes-Landázuri,<sup>a,b</sup> and Steven D. Emslie<sup>g</sup>

<sup>a</sup>Colegio de Ciencias Biológicas y Ambientales, Universidad San Francisco de Quito, Quito, Ecuador

<sup>b</sup>Galápagos Science Center, Puerto Baquerizo Moreno, Ecuador

<sup>c</sup>Department of Marine Sciences, University of South Alabama, Mobile, Alabama, USA

<sup>d</sup>Institute for the Oceans and Fisheries, University of British Columbia, Vancouver, British Columbia, Canada

<sup>e</sup>Upper Midwest Water Science Center, US Geological Survey, Middleton, Wisconsin, USA

<sup>f</sup>Harvard T.H. Chan School of Public Health, Harvard University, Cambridge, Massachusetts, USA

<sup>g</sup>Department of Biology and Marine Biology, University of North Carolina, Wilmington, North Carolina, USA

**Abstract:** We examined how dietary factors recorded by C and N influence Hg uptake in 347 individuals of yellowfin tuna (*Thunnus albacares*), an important subsistence resource from the Galápagos Marine Reserve (Ecuador) and the Ecuadorian mainland coast in 2015–2016. We found no differences in total Hg (THg) measured in red muscle between the two regions and no seasonal differences, likely due to the age of the fish and slow elimination rates of Hg. Our THg concentrations are comparable to those of other studies in the Pacific (0.20–9.60 mg/kg wet wt), but a subset of individuals exhibited the highest Hg concentrations yet reported in yellowfin tuna. Mercury isotope values differed between  $\Delta^{199}\text{Hg}$  and  $\delta^{202}\text{Hg}$  in both regions ( $\Delta^{199}\text{Hg} = 2.86 \pm 0.04\text{‰}$  vs.  $\Delta^{199}\text{Hg} = 2.33 \pm 0.07\text{‰}$ ), likely related to shifting food webs and differing photochemical processing of Hg prior to entry into the food web. There were significantly lower values of both  $\delta^{15}\text{N}$  and  $\delta^{13}\text{C}$  in tuna from Galápagos Marine Reserve ( $\delta^{15}\text{N}$ : 8.5–14.2‰,  $\delta^{13}\text{C}$ : –18.5 to –16.1‰) compared with those from the Ecuadorian mainland coast ( $\delta^{15}\text{N}$ : 8.3–14.4‰,  $\delta^{13}\text{C}$ : –19.4 to –11.9‰), of which  $\delta^{13}\text{C}$  values suggest spatially constrained movements of tuna. Results from the pooled analysis, without considering region, indicated that variations in  $\delta^{13}\text{C}$  and  $\delta^{15}\text{N}$  values tracked changes of Hg stable isotopes. Our data indicate that the individual tuna we used were resident fish of each region and were heavily influenced by upwellings related to the eastern Pacific oxygen minimum zone and the Humboldt Current System. The isotopes C, N, and Hg reflect foraging behavior mainly on epipelagic prey in shallow waters and that food web shifts drive Hg variations between these populations of tuna. *Environ Toxicol Chem* 2022;00:1–13. © 2022 SETAC

**Keywords:** Isotopes; carbon; nitrogen; mercury; yellowfin tuna

## INTRODUCTION

Mercury (Hg) is a toxic metal that is globally distributed due to numerous natural and anthropogenic sources such as geological weathering, gold mining, coal combustion, and industrial discharges (Le Croizier et al., 2019). The oceans receive approximately 90% of Hg through atmospheric deposition, which is predominantly from anthropogenic influences (Chen et al., 2012). The most toxic form of this element is

methylmercury (MeHg), a neurotoxicant that can form in anoxic pockets of the water column or nearshore zones due to microbial processing and can then further bioaccumulate up the food web (Drevnick et al., 2015). High levels of MeHg in fish can lead to adverse effects on growth and survival, particularly in larger piscivorous species (Scheuhammer et al., 2015). Various studies have reported severe physiological effects of MeHg exposure in wildlife and in humans (Bosch et al., 2016), which is of great concern for ocean fisheries that are utilized worldwide.

Like other oceans, the Pacific is facing several environmental challenges including pollution, overexploitation of fisheries, destruction of habitats, and acidification (Chen & Li, 2019). Several studies have reported moderate to high increases in

This article includes online-only Supporting Information.

\* Address correspondence to laiajulianamu@gmail.com

Published online 17 August 2022 in Wiley Online Library

(wileyonlinelibrary.com).

DOI: 10.1002/etc.5458

MeHg concentrations in yellowfin tuna (*Thunnus albacares*) in the Pacific Ocean during the last decades (Drevnick et al., 2015). On the other hand, a recent study (Médiéu et al., 2021) reported that only 0.6% of the samples of yellowfin tuna in their data set were above the food safety guideline (i.e., 1 ppm or mg/kg wet wt according to the guide for fish consumption established by the Inter-Organization Programme for the Sound Management of Chemicals, 2008) and did not find significant increasing decadal trends of Hg concentrations in yellowfin tuna, suggesting the probable existence of distinct ocean patterns of Hg. Tuna contamination is of particular concern for global human health due to its large-scale global exports (Pauly & Zeller, 2016) as well as its frequent consumption by subsistence communities, particularly in developing countries such as Ecuador where it constitutes an important source of protein (Galland et al., 2016).

Island ecosystems of the United Nations Educational, Scientific and Cultural Organization World Heritage Site, the Galápagos Islands, are affected by global and regional anthropogenic pollution and chemical releases despite their remoteness (Alava & Ross, 2018). However, little is known about Hg levels in the Galápagos and other island ecosystems. In the Galápagos Islands and the Ecuadorian mainland coast, metal assessments have been reported at high concentrations for various toxic elements (Al, B, Ba, Cd, Ni, Pb, and Sr) above safety guidelines and regional values for a few large pelagic and demersal fishes (i.e., yellowfin tuna; common dolphinfish or “dorado,” *Coryphaena hippurus*; palm ruff, *Seriola lalandi*), and several demersal fish species (South Pacific hake, *Merluccius gayi*; Peruvian weakfish, *Cynoscion analis*; rock basses, *Paralabrax* spp.; ocean whitefish, *Caulolatilus princeps*; and sailfin grouper, *Mycteroperca olfax* (Franco-Fuentes et al., 2021). In particular, Maurice et al. (2021) recently reported that differences in Hg isotope values were a function of feeding area and that high Hg concentrations were present due to specific feeding regimes in several species of pelagic sharks from the Galápagos Marine Reserve and surrounding oceanic waters.

Isotope tracer methods have been applied to examine the influence of food web dynamics and changes in Hg sources because these relate to Hg burdens in pelagic fish. Nitrogen isotopes ( $\delta^{15}\text{N}$ ) have been used to examine Hg variation as a function of trophic level, and carbon isotopes ( $\delta^{13}\text{C}$ ) allow discrimination between oceanic versus coastal and pelagic or demersal habitats in marine fishes and help us to understand the role of foraging habitat in Hg bioaccumulation (Pethybridge et al., 2015). Similar to carbon and nitrogen isotopes, Hg isotopes undergo mass-dependent fractionation (MDF), which has been leveraged to examine source changes in biological tissue, often recorded as  $\delta^{202}\text{Hg}$  (Janssen et al., 2019), and mass-independent fractionation (MIF) including the odd isotopes  $\Delta^{199}\text{Hg}$  and  $\Delta^{201}\text{Hg}$ , mainly driven by photochemical reactions in the environment (Bergquist & Blum, 2007; Blum & Bergquist, 2007). Patterns in MIF have been used in ocean food webs to assess foraging depth, with decreasing  $\Delta^{199}\text{Hg}$  values associated with decreasing light penetration with depth and the

influence of epipelagic Hg sources on mesopelagic or deep sea consumers (Blum et al., 2013, 2020). Also occurring in  $\Delta^{200}\text{Hg}$ , MIF has been attributed to atmospheric pools of Hg such as precipitation and gaseous elemental forms (Blum et al., 2013), allowing for an additional vector of source identification.

In the present study we provide the first assessment of Hg concentrations and C, N, and Hg isotope values in yellowfin tuna during the warm and cold seasons in the Galápagos Marine Reserve and waters off the Ecuadorian mainland coast. Our primary objectives were to determine whether individuals from the two regions differ in Hg concentrations and isotopic values ( $\delta^{202}\text{Hg}$ ,  $\Delta^{199}\text{Hg}$ , and  $\Delta^{200}\text{Hg}$ ), to infer sources (natural/geogenic vs. anthropogenic) of the Hg, and to explore possible relationships with Hg exposure as a function of trophic position, using bulk stable isotopes ( $\delta^{13}\text{C}$  and  $\delta^{15}\text{N}$ ). It is vital to understand the dynamics of Hg bioaccumulation and determine ecological factors that may be driving elevated Hg concentrations in yellowfin tuna given their importance to fisheries in the Pacific Ocean.

## MATERIALS AND METHODS

### Sample collection

Sampling was conducted in two regions, the Galápagos Marine Reserve and along the Ecuadorian mainland coast (Figure 1). These two regions were chosen because of the influence of different ocean currents and also the habitat use and distribution of yellowfin tuna how according to the last movement assessment in the region and their attraction to islands (Schaefer & Fuller, 2022). The Galápagos Marine Reserve samples were obtained at two sites, the ports of San Cristóbal Island and Santa Cruz Island, where local fishermen provided access to their catch after their arrival at the ports. At the Ecuadorian mainland coast, samples were obtained at the port of Santa Rosa, Santa Elena province. Samples were collected during the cold season of 2015 (July and August) and the warm season of 2016 (January and February; Figure 1). Therefore, to explore seasonal effects on tuna size, total mercury (THg), and isotopic values that could result from the influence of the Humboldt (cold) and Equatorial (warm) currents, a total of 347 samples was obtained, including 104 from the Galápagos Marine Reserve and 46 from the Ecuadorian mainland coast during the cold season in 2015, and 139 samples from the Galápagos Marine Reserve and 58 from the Ecuadorian mainland coast during the warm season of 2016. Each tuna sampled was individually measured for standard length (tip of snout to edge of caudal peduncle keel) and, using a porcelain knife, we collected approximately 2 g (wet wt) of red muscle from the top mid-dorsal line. The tissue was immediately stored in Eppendorf tubes on ice at  $-8^{\circ}\text{C}$ . For 134 individuals whose heads had been removed by the fishermen prior to their arrival to the port, the standard length was predicted by a linear regression applied to 65 individuals in which both the standard length and the headless length were measured. Only tuna from artisanal fisheries and known capture sites were sampled and measured to ensure that the

## Fishing zones of Mainland Ecuador and Galápagos Marine Reserve

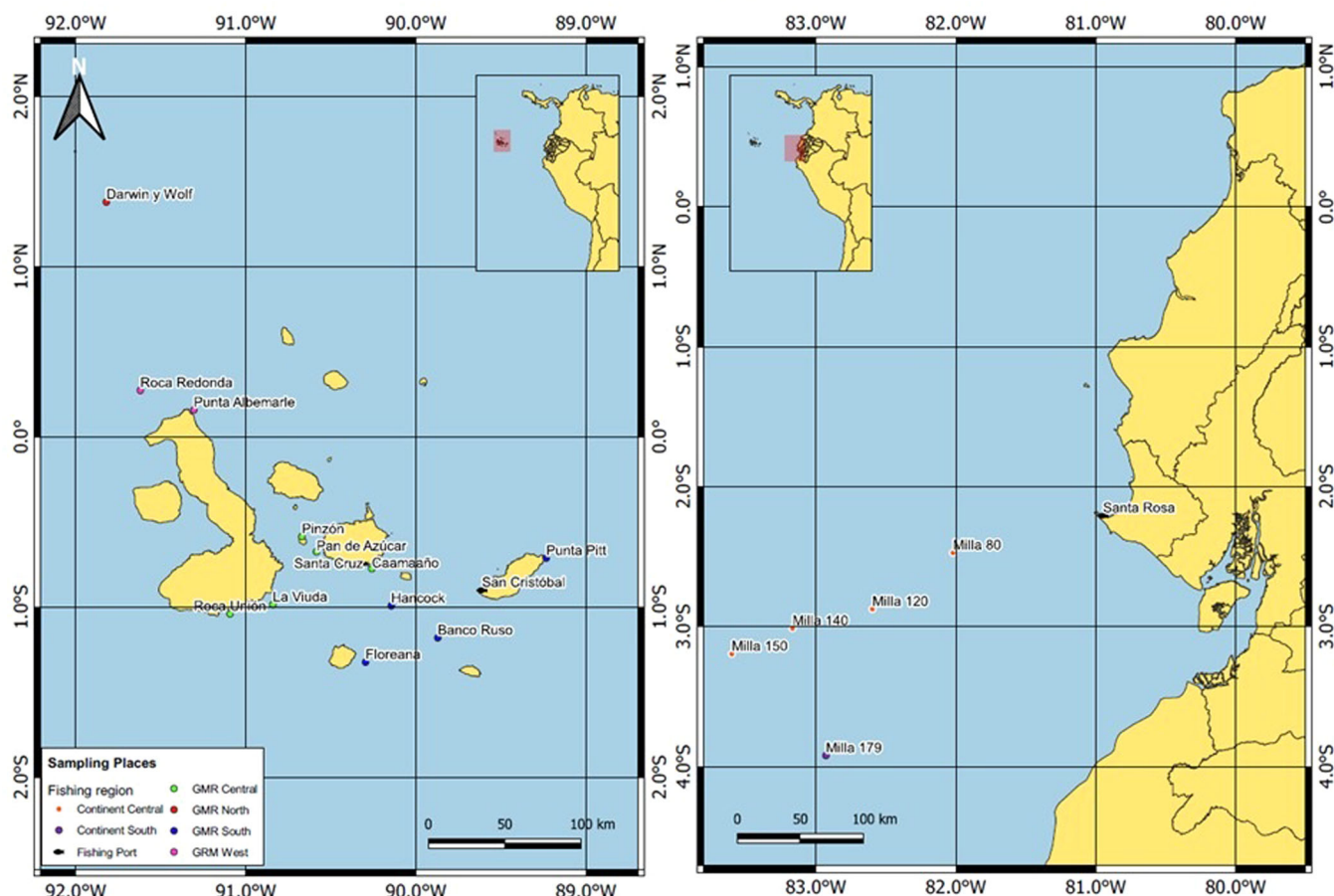


**FIGURE 1:** Map of fishing zones showing the sampling sites in marine waters around the Galápagos Marine Reserve (left) and off the Ecuadorian mainland coast (right). The Galápagos Islands are located 1000 km from the Ecuadorian coast.

tuna came from two different regions (Ecuadorian mainland coast and Galápagos Marine Reserve).

### Hg analyses

All samples were freeze-dried for 24 h to remove moisture using a TFD5503 Bench-Top freeze dryer (LABCONCO), followed by homogenization using a mortar and pestle at the Agricultural Biotechnology laboratory of the Universidad San Francisco de Quito (Ecuador). Measurements of THg in tissues were performed on a Milestone DMA-80 Hg analyzer at the University of North Carolina Wilmington (USA). Each set of 20 samples was preceded and followed by two method blanks, a sample blank, and two samples each of standard reference material (DORM-4 and DOLT-5 from fish protein and dogfish liver, respectively, certified by the National Research Council, Canada). Mean (weighted) percent recovery of certified reference material was 96.6% (DORM-4 = 99.9%, DOLT-5 = 93.3%, 0.02 g). Most of the THg measured in these tuna was assumed to be MeHg because it has been shown that between 90% and 100% of the total Hg found in muscle samples from the dorsal

musculature, especially apex predators, is in this form (Madigan et al., 2018). The Hg concentration values obtained in dry weight were converted to wet weight values to compare our results with those of other studies and with the tolerable intake values internationally approved by the World Health Organization, which are estimated on a wet weight basis. The transformation of the dry weight to wet weight values was performed using a moisture percentage of 70% as reported by Teffer et al. (2014) for yellowfin tuna.

### Hg stable isotopes

A subset of tuna samples from the Galápagos Marine Reserve ( $n = 10$ ) and the Ecuadorian mainland coast ( $n = 10$ ) was selected randomly for Hg isotope analysis at the US Geological Survey (USGS) Mercury Research Laboratory (Middleton, WI). Tissue samples were digested in concentrated nitric acid (100 mg of tissue/1 ml of acid) and heated at more than 90 °C for 8 h. Following the initial heating, samples were amended with bromine monochloride to a final concentration of 10% prior to heating for an additional 2–3 h. Prior to isotope

analysis, samples were diluted with ultra pure water to a final acid content of 20%. Isotope ratios were measured using a Neptune Plus multicollector inductively coupled plasma–mass spectrometer to stannous chloride reduction in a custom-designed gas–liquid separator (Yin et al., 2016). Samples were analyzed using standard bracketing with National Institute of Standards (NIST) 3133 and measured simultaneously with aerosol introduction of Tl (NIST 997) to correct for instrument bias (Blum & Bergquist, 2007). During analysis six Hg isotopes were monitored ( $^{198}\text{Hg}$ ,  $^{199}\text{Hg}$ ,  $^{200}\text{Hg}$ ,  $^{201}\text{Hg}$ ,  $^{202}\text{Hg}$ , and  $^{204}\text{Hg}$ ) simultaneously with thallium ( $^{203}\text{Tl}$  and  $^{205}\text{Tl}$ ). Isotope values were calculated based on a convention such that MDF is expressed in terms of  $\delta^{\text{xxx}}\text{Hg}$  and calculated as:

$$\delta^{\text{xxx}}\text{Hg}(\%) = \left\{ \frac{\text{xxxHg}/^{198}\text{Hg}_{\text{sample}}}{(\text{xxxHg}/^{198}\text{Hg}_{\text{NIST} - 3133}) - 1} \right\} \times 1000 \quad (1)$$

where XXX is used to signify the Hg isotope of interest. Mercury also undergoes MIF of both even and odd isotopes, calculated as:

$$\Delta^{\text{xxx}}\text{Hg} \approx \delta^{\text{xxx}}\text{Hg} - (\delta^{202}\text{Hg} \times \beta) \quad (2)$$

where  $\beta$  represents the mass scaling factor.

A secondary standard (UM Almaden, NIST RM 8610) was measured every 5–10 samples to ensure accuracy and precision ( $\delta^{202}\text{Hg} = -0.51 \pm 0.10$ ;  $\Delta^{199}\text{Hg} = -0.02 \pm 0.06$ ;  $\Delta^{200}\text{Hg} = 0.01 \pm 0.04$ , 2 standard deviation [SD];  $n = 13$ ). In addition, a certified reference material, International Atomic Energy Agency 407 (fish homogenate), was also measured to verify digestion efficiency every 10 samples ( $\delta^{202}\text{Hg} = 0.70 \pm 0.08$ ;  $\Delta^{199}\text{Hg} = 1.05 \pm 0.12$ ;  $\Delta^{200}\text{Hg} = 0.07 \pm 0.04$ , 2 SD;  $n = 4$ ) and agreed with previously published values (Janssen et al., 2019). Finally, a linear correction to remove fractionation associated with photochemistry was applied using the method outlined in Blum et al. (2013), these values were termed  $\delta^{202}\text{Hg}_{\text{COR}}$ . The values obtained were compared with those for other oceanic fish collected in the northern (Blum et al., 2013) and western Pacific (Madigan et al., 2018) and fish collected in the coastal areas (Balogh et al., 2015; Liu et al., 2007; Liu et al., 2018; Senn et al., 2010).

### Carbon and nitrogen stable isotope analysis

Stable isotope abundances are expressed in  $\delta$  notation in per mil units (‰), according to the following equation:

$$\delta X = \left[ \left( \frac{R_{\text{sample}}}{R_{\text{standard}}} \right) - 1 \right] \times 1000 \quad (3)$$

where X is  $^{13}\text{C}$  or  $^{15}\text{N}$  and v is the corresponding ratio  $^{13}\text{C}/^{12}\text{C}$  or  $^{15}\text{N}/^{14}\text{N}$ . The R standard values were based on the Vienna PeeDee Belemnite for  $^{13}\text{C}$  and atmospheric  $\text{N}_2$  for  $^{15}\text{N}$ .

For each analysis (carbon and nitrogen isotopes), 0.4–0.6 mg dry weight of each sample was used. The first step was incineration in a Costech ECS4010 elemental analyzer. Subsequently, stable isotope ratios of nitrogen ( $\delta^{15}\text{N}$ ) and carbon ( $\delta^{13}\text{C}$ ) were analyzed in a Thermo Delta mass

spectrometer (IRMS) at the Center for Marine Science at University of North Carolina Wilmington. The values of nitrogen and carbon were normalized using reference materials. The reference material was depleted and enriched glutamic acid (USGS-40:  $\delta^{13}\text{C} = -26.4\%$ ,  $\delta^{15}\text{N} = -4.5\%$ , USGS-41:  $\delta^{13}\text{C} = 37.6$  ppm,  $\delta^{15}\text{N} = 47.6$  ppm). The precision of the sample, based on a repeated sampling of the reference materials, was 0.1‰ for  $\delta^{13}\text{C}$  and 0.2‰ for  $\delta^{15}\text{N}$ .

We used the equation of Post et al. (2007), tested by Sardenne et al. (2015), in tropical tuna including yellowfin tuna to normalize the results obtained from carbon, which serves as a proxy of both diet and lipid composition. The correction applied for carbon was:

$$\delta^{13}\text{C}_{\text{normalized}} = \delta^{13}\text{C}_{\text{uncorrected}} - 3.32 + 0.99 \times \text{C} : \text{Nuncorrected} \quad (4)$$

### Statistical analysis

We used generalized linear mixed models with gamma distribution (and log link) because the data did not meet normality assumptions and all numerical variables were positively skewed. Due to the spatial–temporal sampling scheme within each region, different locations were sampled during the warm and the cool seasons; overall seasonal effects were analyzed separately from models that explored spatial (region, season, location) effects and the relationship among THg,  $\delta^{13}\text{C}$ , and  $\delta^{15}\text{N}$  values and tuna size (standard length).

All analyses were performed in R Ver 3.6.1 (R Studio Team, 2020). All equations and raw data are located in the supporting information, Tables S1–S4.

## RESULTS

Our results showed no differences in THg between regions ( $t = 0.74$ ,  $p = 0.45$ ; Table 1), with a mean  $\pm$  SD for the Ecuadorian mainland coast of  $1.11 \pm 1.67$  ppm wet weight and  $1.72 \pm 1.11$  ppm wet weight in the Galápagos Marine Reserve. The  $\delta^{13}\text{C}$  was lower in the Galápagos Marine Reserve ( $b = -0.526$  [−0.80 to −0.25]  $t = 3.71$ ,  $p < 0.001$ ), with a mean of  $-17.66 \pm 0.33\%$  wet weight, whereas the mean in the Ecuadorian mainland coast was  $-15.10 \pm 1.45\%$  wet weight. The  $\delta^{15}\text{N}$  was lower in the Galápagos Marine Reserve ( $b = -0.046$  [−0.085 to −0.006]  $t = 2.27$ ,  $p = 0.023$ ), with a mean of  $11.15 \pm 0.85\%$  wet weight versus a mean in the Ecuadorian mainland coast of  $11.43 \pm 1.18\%$  wet weight. Tuna length did not differ between regions ( $t = 0.88$ ,  $p = 0.37$ ). The average tuna length in the Ecuadorian mainland coast was  $63.71 \pm 26.65$  cm, and in the Galápagos Marine Reserve it was  $90.05 \pm 25.08$  cm (Supporting Information, Figure S1).

A difference in THg was not indicated by our seasonal analyses ( $t = 0.88$ ,  $p = 0.37$ ; Table 2). Mean Hg was  $1.45 \pm 1.34$  mg/kg wet weight during the cold season and  $1.65 \pm 1.32$  mg/kg wet weight during the warm season. Carbon had a similar behavior, with no differences between seasons ( $t = 0.48$ ,  $p = 0.62$ ), a mean of  $-17.0\%$  (SD = 1.15) wet weight during the cold season, and  $-16.9 \pm 1.63\%$  wet weight during the warm

**TABLE 1:** Descriptive statistics by regions

	Ecuadorian mainland			Galápagos Marine Reserve				
	Central (n = 74)	South (n = 69)	Overall (n = 102)	Central (n = 78)	North (n = 20)	South (n = 57)	West (n = 45)	Overall (n = 241)
THg (ppm wet wt)								
Mean (SD)	1.55 (1.30)	2.44 (1.22)	1.11 (1.67)	1.36 (0.42)	1.26 (0.51)	0.71 (0.49)	1.62 (2.37)	1.72 (1.11)
Median (min, max)	1.20 (0.60, 9.60)	2.40 (0.4, 7.30)	0.60 (0.20, 9.40)	1.35 (0.30, 2.20)	1.10 (0.50, 2.0)	0.60 (0.20, 3.10)	0.60 (0.50, 9.40)	1.50 (0.30, 9.60)
$\delta^{15}\text{N}$								
Mean (SD)	10.7 (0.79)	11.5 (0.74)	11.4 (1.18)	10.7 (0.84)	11.4 (0.52)	11.9 (0.76)	10.9 (1.39)	11.0 (0.85)
Median (min, max)	10.8 (8.50, 12.5)	11.5 (8.60, 14.2)	11.7 (8.30, 14.4)	10.6 (9.0, 13.1)	11.3 (10.6, 12.5)	11.8 (10.1, 13.8)	10.9 (8.30, 14.4)	11.1 (8.50, 14.2)
$\delta^{13}\text{C}$								
Mean (SD)	-17.7 (0.27)	-17.6 (0.36)	-15.1 (1.45)	-17.7 (0.35)	-17.7 (0.33)	-14.7 (1.57)	-15.5 (1.16)	-17.7 (0.32)
Median (min, max)	-17.7 (-18.5, -16.9)	-17.7 (-18.3, -16.1)	-15.1 (-19.4, -11.9)	-17.7 (-18.5, -16.7)	-17.7 (-18.3, -17.1)	-14.1 (-17.8, -11.9)	-15.3 (-19.4, -13.7)	-17.7 (-18.5, -16.1)
Standard length (cm)								
Mean (SD)	75.5 (0.266)	116 (0.22)	63.7 (26.6)	83.1 (17.8)	80.7 (17.6)	60.5 (5.11)	67.8 (39.6)	90 (25.1)
Median (min, max)	74.0 (46.6, 133)	117 (64.0, 171)	61 (41.0, 200)	77.0 (56.0, 131)	74.5 (59.0, 118)	62.0 (43, 67)	53.0 (41, 200)	78 (46, 171)

ppm = parts per million; SD = standard deviation; THg = total mercury.

**TABLE 2:** Descriptive statistics by seasons

	Season		
	Cold (n = 148)	Warm (n = 343)	Overall (n = 102)
THg (ppm wet wt)			
Mean (SD)	1.45 (1.34)	1.61 (1.32)	1.54 (1.33)
Median	1.25	1.10	1.20
(min, max)	(0.30, 9.40)	(0.20, 9.60)	(0.20, 9.60)
$\delta^{15}\text{N}$ (‰)			
Mean (SD)	10.6 (0.99)	11.6 (0.73)	11.1 (0.97)
Median	10.4	11.5	11.2
(min, max)	(8.30, 14.4)	(8.60, 14.2)	(8.30, 14.4)
$\delta^{13}\text{C}$ (‰)			
Mean (SD)	-17.0 (1.15)	-16.9 (1.63)	-16.9 (1.44)
Median	-17.5	-17.6	-17.5
(min, max)	(-19.4, -13.7)	(-18.5, -11.9)	(-19.4, -11.9)
Standard length (cm)			
Mean (SD)	75.9 (25.6)	87 (29.2)	82.2 (28.2)
Median	74 (41, 200)	78 (43, 171)	74 (41, 200)
(min, max)			

ppm = parts per million; SD = standard deviation; THg = total mercury.

season. Nitrogen was higher during the warm season ( $b = 0.09$ , [0.06 to 0.12]  $t = 6.92$ ,  $p > 0.001$ ), with a mean of  $11.6 \pm \% 0.73$  wet weight, whereas during the cold season the mean was  $10.6 \pm 0.99\%$  wet weight. Between seasons, there was no difference in the standard length of the fish ( $t = 0.02$ ,  $p = 0.97$ ). The mean size of tuna during the cold season was  $75.9 \pm 25.6$  cm, whereas during the warm season, it was  $87 \pm 29.2$  cm (Figure 2).

According to our model, a seasonal analysis within each region showed that THg was lower in the Ecuadorian mainland coast during the warm season ( $b = -0.826$  [-1.37 to -0.27]  $t = 2.94$ ,  $p = 0.003$ ), whereas there was no detectable effect in the Galápagos Marine Reserve ( $t = 1.21$ ,  $p = 0.22$ ). No evidence of seasonal effect within regions was indicated in  $\delta^{13}\text{C}$  (Galápagos Marine Reserve:  $t = 1.338$ ,  $p = 0.18$ ; Ecuadorian mainland coast:  $t = 0.99$ ,  $p = 0.36$ ). The  $\delta^{13}\text{C}$  was higher during the warm season in both regions, that is, in the Ecuadorian mainland coast ( $b = 0.08$  [0.042–0.128]  $t = 3.86$ ,  $p < 0.001$ ) and the Galápagos Marine Reserve ( $b = 0.09$  [0.07–0.123]  $t = 7.18$ ,  $p < 0.001$ ). The standard length showed no seasonal variation within regions (Galápagos Marine Reserve:  $t = 0.64$ ,  $p = 0.52$ ; Ecuadorian mainland coast:  $t = 0.66$ ,  $p = 0.51$ ). Finally, no association was found between THg levels and  $\delta^{15}\text{N}$  ( $t = 1.89$ ,  $p = 0.06$ ),  $\delta^{13}\text{C}$  ( $t = 0.87$ ,  $p = 0.38$ ), or tuna size ( $t = 1.72$ ,  $p = 0.09$ ; Figure 2).

### Hg stable isotopes

All fish from our study had Hg isotope values comparable to those of previous studies examining fish tissue in the Pacific Ocean (Blum et al., 2013; Madigan et al., 2018) as well as coastal regions across different ocean basins (Balogh et al., 2015; Liu et al., 2007; Liu et al., 2018; Senn et al., 2010; Figure 3). Yellowfin tuna samples from the Galápagos Marine Reserve exhibited higher  $\Delta^{199}\text{Hg}$  than those from the

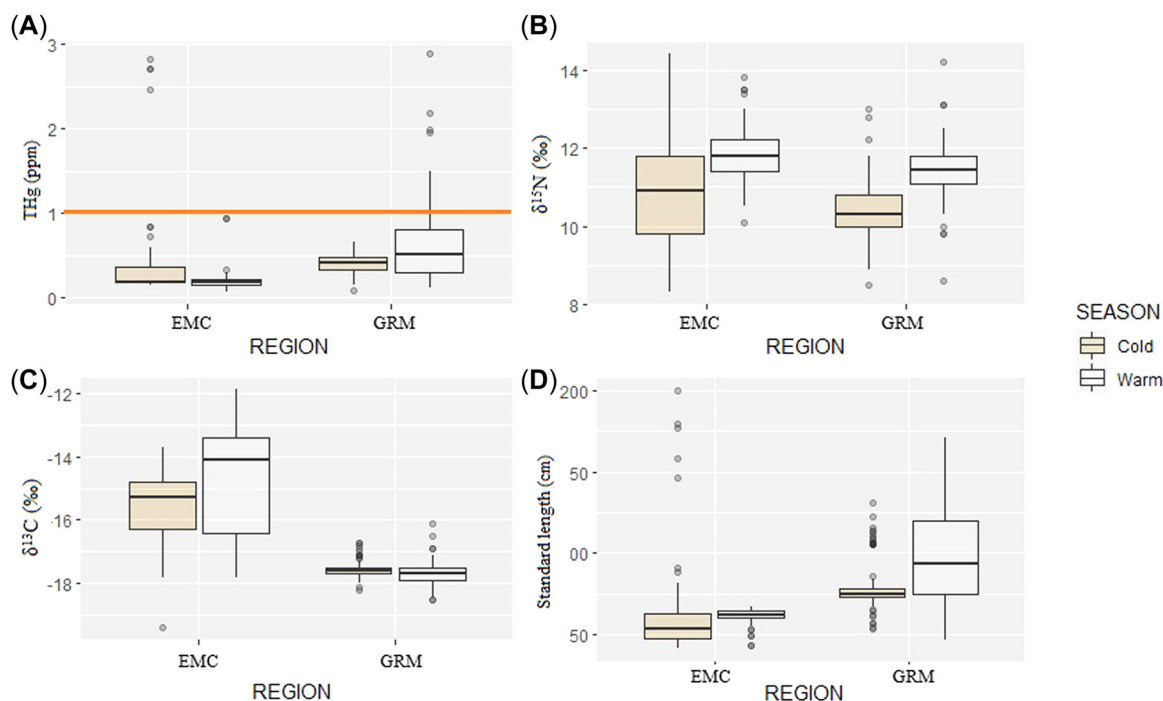


**FIGURE 2:** Boxplots of total mercury (THg; **A**),  $\delta^{15}\text{N}$  (**B**),  $\delta^{13}\text{C}$  (**C**), and standard length (**D**) of yellowfin tuna by region and season. White is warm, and yellow is cold. EMC = Ecuadorian mainland coast; GMR = Galápagos Marine Reserve.

Ecuadorian mainland coast ( $\Delta^{199}\text{Hg} = 2.86 \pm 0.04\%$  vs.  $\Delta^{199}\text{Hg} = 2.33 \pm 0.07\%$ ;  $W = 4$ ,  $p = 0.00012$ ). The same trend was observed for MDF tracers ( $\delta^{202}\text{Hg} = 0.79 \pm 0.03\%$  vs.  $\delta^{202}\text{Hg} = 0.61 \pm 0.05\%$ ;  $W = 18.5$ ,  $p = 0.01$ ), although it is noted that tuna from the Ecuadorian mainland coast have a larger range for this isotopic signature (Figure 3). The photochemical slope ( $\Delta^{199}\text{Hg}/\Delta^{201}\text{Hg}$ ) observed in these tuna fish was  $1.20 \pm 0.04$  (York regression, 1 SD), was in line with experimental studies of photochemical demethylation, which is typically assessed to have a slope of 1.3 (Motta et al., 2020).

Another method to examine the different potential sources of Hg to these populations is by using a mathematical correction to assess the isotope value of  $\delta^{202}\text{Hg}$  prior to water column processing, as outlined elsewhere (Blum et al., 2013; Janssen et al., 2019). Although this approach has several caveats, specifically related to the numerical relation of  $\delta^{202}\text{Hg}$  and  $\Delta^{199}\text{Hg}$  in the presence of varying dissolved organic carbon contents (Bergquist & Blum, 2007), the tuna in our study are generally exposed to similar marine carbon sources that allow for intercomparison between the Galápagos Marine Reserve

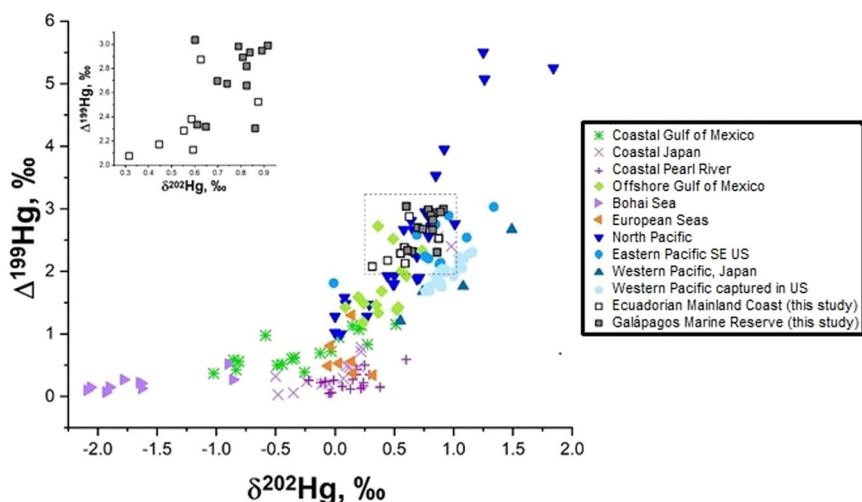


**FIGURE 3:** Comparison of Hg isotope values  $\delta^{202}\text{Hg}$  and  $\Delta^{199}\text{Hg}$  between oceanic and coastal fish. Samples from the present study are shown in the inset chart (white and gray squares for Ecuadorian Mainland Coast [EMC] and Galápagos Marine Reserve [GMR], respectively). Data are referenced from the following: coastal and offshore Gulf of Mexico (Senn et al., 2010); coastal Japan (Balogh et al., 2015); coastal Pearl River (Yin et al., 2016); Bohai Sea (Liu et al., 2018), European Seas (Cransveld et al., 2017); North Pacific (Blum et al., 2013); and Eastern and Western Pacific (Madigan et al., 2018).

and the Ecuadorian mainland coast groups. Using this correction, the  $\delta^{202}\text{Hg}_{\text{COR}}$  values for the Ecuadorian mainland coast ( $\delta^{202}\text{Hg}_{\text{COR}} = -0.35 \pm 0.15\text{‰}$ ,  $n = 10$ ) and the Galápagos Marine Reserve ( $\delta^{202}\text{Hg}_{\text{COR}} = -0.38 \pm 0.10\text{‰}$ ,  $n = 10$ ) were not statistically different, although some variation was observed between individuals, indicating that there is no source difference prior to photochemical processing of Hg. All the tuna sampled also had positive  $\Delta^{200}\text{Hg}$  signatures, ranging from 0.04‰ to 0.15‰. Positive values of  $\Delta^{200}\text{Hg}$  have been recorded in precipitation and have been further used as conservative tracers for atmospheric sources of Hg. No fractionation of  $\Delta^{200}\text{Hg}$  has been observed by photochemical demethylation (Bergquist & Blum, 2007) in the water column or metabolic processes that can affect other Hg isotopes (Feng et al., 2015), indicating that  $\Delta^{200}\text{Hg}$  in the tuna are derived from an atmospheric source of Hg.

### Hg isotopes in combination with $\delta^{15}\text{N}$ and $\delta^{13}\text{C}$

Correlations among  $\delta^{15}\text{N}$ ,  $\delta^{13}\text{C}$ , and Hg isotopic signatures were investigated to identify the most important factors influencing Hg accumulation in yellowfin tuna from the Galápagos Marine Reserve and the Ecuadorian mainland coast, specifically the potential relation between Hg and C sources. No significant trends were found between  $\Delta^{199}\text{Hg}$  and  $\delta^{15}\text{N}$  ( $\rho = -0.43$ ,  $p = 0.21$  in the Galápagos Marine Reserve and  $\rho = -0.22$ ,  $p = 0.53$  in the Ecuadorian mainland coast), or  $\delta^{202}\text{Hg}$  and  $\delta^{15}\text{N}$  ( $\rho = 0.24$ ,  $p = 0.48$  in the Galápagos Marine Reserve and  $\rho = -0.31$ ,  $p = 0.37$  in the Ecuadorian mainland coast) in yellowfin tuna from either the Galápagos Marine Reserve or the Ecuadorian mainland coast.

Similarly, no significant trends were found between  $\Delta^{199}\text{Hg}$  and  $\delta^{13}\text{C}$  values ( $\rho = 0.21$ ,  $p = 0.55$  in the Galápagos Marine

Reserve and  $\rho = -0.12$ ,  $p = 0.73$  in the Ecuadorian mainland coast), and  $\delta^{202}\text{Hg}$  and  $\delta^{13}\text{C}$  ( $\rho = 0.15$ ,  $p = 0.66$  in the Galápagos Marine Reserve and  $\rho = -0.12$ ,  $p = 0.73$  in the Ecuadorian mainland coast). Our analyses between  $\Delta^{199}\text{Hg}$  and THg showed no significant trends in the Galápagos Marine Reserve ( $\rho = -0.11$ ,  $p = 0.75$ ) or the Ecuadorian mainland coast ( $\rho = 0.44$ ,  $p = 0.20$ ). The same occurred for  $\delta^{202}\text{Hg}$  and THg, in which no significant trends were found in either site ( $\rho = -0.09$ ,  $p = 0.8$  in the Galápagos Marine Reserve, and  $\rho = 0.56$ ,  $p = 0.08$  in the Ecuadorian mainland coast).

Combining both the Galápagos Marine Reserve and the Ecuadorian mainland coast data, we found positive relationships between  $\Delta^{199}\text{Hg}$  and THg ( $\rho = 0.46$ ,  $p = 0.04$ ), and between  $\delta^{202}\text{Hg}$  and THg ( $\rho = 0.49$ ,  $p = 0.04$ ). Similarly, combining both the Galápagos Marine Reserve and the Ecuadorian mainland coast data to assess the relationship between  $\Delta^{199}\text{Hg}$  and  $\delta^{15}\text{N}$  at a regional scale in the southeastern Pacific Ocean, we found a significant negative relationship ( $\rho = -0.63$ ,  $p = 0.0037$ ) between  $\Delta^{199}\text{Hg}$  and  $\delta^{15}\text{N}$ , but no significant relationship ( $\rho = -0.28$ ,  $p = 0.23$ ) between  $\delta^{202}\text{Hg}$  and  $\delta^{15}\text{N}$ . In a pooled analysis of both the Galápagos Marine Reserve and the Ecuadorian mainland coast data, we found significant negative relationships between  $\Delta^{199}\text{Hg}$  and  $\delta^{13}\text{C}$  ( $\rho = -0.64$ ,  $p = 0.003$ ), and no significant relationships between  $\delta^{202}\text{Hg}$  and  $\delta^{13}\text{C}$  ( $\rho = -0.19$ ,  $p = 0.42$ ; Figure 4).

## DISCUSSION

### Factors influencing Hg concentrations in yellowfin tuna

The lack of inter-regional and seasonal differences, and size influences (standard length) in THg concentrations measured in yellowfin tuna from the Galápagos Marine

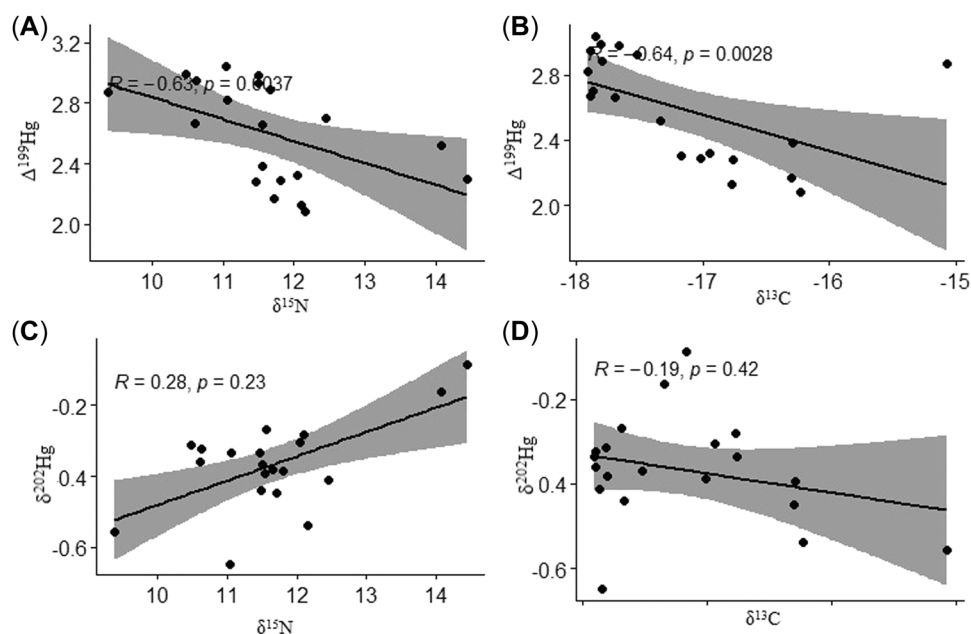


**FIGURE 4:** Relationships between mercury isotopes ( $\Delta^{199}\text{Hg}$ ,  $\delta^{202}\text{Hg}$ ) and stable isotopes of nitrogen and carbon ( $\delta^{15}\text{N}$ ,  $\delta^{13}\text{C}$ ) measured in yellowfin tuna sampled in waters of the Galápagos Marine Reserve and the Ecuadorian mainland coast. Correlation of (A)  $\Delta^{199}\text{Hg}$  with  $\delta^{15}\text{N}$ , (B)  $\Delta^{199}\text{Hg}$  with C, (C)  $\delta^{202}\text{Hg}$  with  $\delta^{15}\text{N}$ , and (D)  $\delta^{202}\text{Hg}$  with  $\delta^{13}\text{C}$ .

Reserve and the Ecuadorian mainland coast could be explained by similar long-term exposure and accumulation of MeHg over the lifetime of the individuals or other biological factors such as size, trophic position, migration pattern, growth, and prey type abundance (which varies or depends on the environment; Tseng et al., 2021). Although some recent tuna studies have demonstrated a relationship between age/size and THg (Tseng et al., 2021), in our study no significant relationships were observed between standard length and THg (Supporting Information, Figure S1). One of the principal reasons is probably that our samples were fishing-dependent, and most of the tuna sizes ranged from 55 to 83 cm due to the artisanal fishing gear used.

Some studies have reported regional residency based on Hg concentrations, showing that populations could be separated because yellowfin tuna accumulate Hg from their area of residence or habitat use (Graham et al., 2010; Houssard et al., 2017; Lorrain et al., 2015). These studies support research using satellite marks that indicate yellowfin tuna are restricted to an area with a radius of approximately 1852 km (Schaefer & Fuller, 2022; Schaefer et al., 2014). Although we found a difference between Hg isotopic signatures between both locations, which suggests a distinction of foraging sites, it is possible that the sampled individuals might have inhabited the entire region, because we found no differences in THg concentration between tuna from the Ecuadorian mainland coast or the Galápagos Marine Reserve and because the areas where the fish were caught are only separated by approximately 1500 km (Muñoz-Abril et al., 2022). Likewise, as previously stated, the favorable oceanographic conditions (i.e., upwellings providing food) would allow individuals to have access to stable resources and permanently inhabit this area. Variations in  $\Delta^{199}\text{Hg}$  are likely derived from photochemical degradation of MeHg in the water column, as has been observed in laboratory studies (Bergquist & Blum, 2007), as well as in other oceanic fish (Madigan et al., 2018), indicating that there are differences in Hg processing between the Galápagos Marine Reserve and the Ecuadorian mainland coast regions that may relate to upwelling zones.

The Eastern Pacific Ocean is one of the most productive ecosystems on the earth, primarily due to the influence of the Humboldt Current System off Peru, which produces the largest amount of fish/unit area in the world, or approximately 10% of the world fish catch in an area equivalent to 0.1% of the world ocean surface (Chavez et al., 2008). Due to sinking and decay of primary productivity at the surface, this area of the Pacific Ocean is one of the largest oxygen minimum zones in the world (Chavez et al., 2008). The anaerobic bacteria, the low dissolved oxygen levels, and the upwelling condition in this area produce MeHg, and some authors have suggested there are high concentrations of it in the Pacific Ocean (Bowman et al., 2020; Houssard et al., 2019; Kraepiel et al., 2003). According to Drevnick et al. (2015), Hg concentrations in Hawaii, located in the North Pacific Ocean, have shown an increase in MeHg due to anthropogenic forces. As expected for a marine top predator, Houssard et al. (2019) reported concentrations of Hg between 0.05 and 5.1 mg/kg wet weight in yellowfin tuna from

the Western and Central Pacific Ocean (Australia to Pitcairn Islands) during 2001–2015, and Chen and Li (2019) reported a range between 0.39 and 2.60 mg/kg wet weight using data from different studies in the Pacific Ocean. Our samples are within the former range, but some individuals showed concentrations of 9.60 mg/kg wet weight, which are higher than reported concentrations in yellowfin tuna in this oceanic region (Drevnick et al., 2015). Drevnick et al. (2015) found a lack of significant changes in MeHg concentrations in consumers at the third trophic level in the area influenced by the Humboldt Current System and suggested that Hg concentrations are explained by the regional effect of the system rather than by a particular climatic or upwelling event. Even though in 2015–2016 a minor El Niño phenomenon was reported, our data suggest that regional differences still control Hg cycling, further supporting the notion that lower Hg concentrations in the Ecuadorian mainland coast during the warm season could be explained by the regional influence of the Humboldt Current System. This conclusion may also explain why no significant relations were found among nitrogen, carbon, and tuna size.

### Variations in trophic status

The isotopic signature of  $\delta^{15}\text{N}$  was observed to be significantly higher throughout the warm season. The yellowfin tuna in our study inhabit areas with specific oceanographic and seasonal conditions that exhibit regional differences in primary productivity and upwelling zones, driving the  $\delta^{15}\text{N}$  isotopic signature in marine species such as pelagic fish and pinniped species inhabiting Galápagos waters (Páez-Rosas et al., 2012, 2020). The southern Tropical Eastern Pacific Ocean is indeed characterized by high primary production because of upwellings of nutrient-rich waters, and the biomass produced is the nourishment of large fishes (Kämpf & Chapman, 2016). As a result of the elevated respiration rates associated with high biological production, the southern Tropical Eastern Pacific Ocean holds the largest worldwide oxygen minimum zone under its thermocline, as mentioned in the previous section, *Factors influencing Hg concentrations in yellowfin tuna* (Fuenzalida et al., 2009; Gilly et al., 2013). Likewise, high ocean temperatures promote the reduction of oxygen, which could ultimately have effects on larger marine organisms including tuna (Oschlies et al., 2018). With the oxygen depleted, anoxic bacteria resort to nitrate ( $\text{NO}_3$ ) as a terminal electron acceptor during denitrification, converting it to nitrite ( $\text{NO}_2$ ; Gruber & Sarmiento, 1997). Due to the preferential uptake of  $\delta^{14}\text{N}$  in  $\text{NO}_3$  by phytoplankton, the remaining  $\text{NO}_3$  is gradually enriched by  $\delta^{15}\text{N}$ , resulting in an inverse relation between the amount of  $\text{NO}_3$  and the values of  $\delta^{15}\text{N}$  (Farrell et al., 1995). Denitrification rates in this region of the Tropical Eastern Pacific Ocean are among the highest in the world. Lorrain et al. (2015) suggest that the  $\delta^{15}\text{N}$  values are explained by isotopic composition at the base of the food web. The differences in  $\delta^{15}\text{N}$  are a consequence of diverse processes such as denitrification in the oxygen minimum zones in upwelling areas, variability in primary production, resource

availability, and different dynamics of N<sub>2</sub> in organisms at low trophic levels (Pethybridge et al., 2018).

Higher  $\delta^{15}\text{N}$  values during the warm season can result from seasonal variability in the intensity of marine upwellings along the Ecuadorian mainland coast. Similar results found by Houssard et al. (2017) and Rafter and Sigman (2016) suggest that nitrogen concentrations vary throughout the southern Tropical Eastern Pacific Ocean, especially within seasons and with water temperatures and, therefore, are not useful for tracing the trophic position of tuna. Other authors have found that it is not possible to use the relationship between  $\delta^{15}\text{N}$  and yellowfin tuna length as an estimator of an individual's trophic level (Ménard et al., 2007). We found the same result: the relationship between those variables was not significant, and those nitrogen values are the result of multiple processes. Nonetheless, measuring  $\delta^{15}\text{N}$  values in top predators is crucial to track the nitrogen dynamics and the sources fueling marine food webs and influencing the general nutrient cycle (Pethybridge et al., 2018).

High  $\delta^{13}\text{C}$  and  $\delta^{15}\text{N}$  values are associated with areas of high primary productivity, whereas low values occur in areas of low productivity (Cherel & Hobson, 2007; Graham et al., 2010; Pethybridge et al., 2018). We found a regional effect on both  $\delta^{15}\text{N}$  and  $\delta^{13}\text{C}$ , with lower values of both isotopes occurring in the Galápagos Marine Reserve despite the occurrence of some “hotspots” for upwellings in the region. Several studies have defined the existence of isoscapes in the southern Tropical Eastern Pacific Ocean, showing a gradual increase of  $\delta^{15}\text{N}$  and  $\delta^{13}\text{C}$  from north to south (Espinoza et al., 2017). The Galápagos Marine Reserve is on the northern edge of this zone, which could explain our findings.

Also, Galápagos Marine Reserve ecosystems are in a transition area affected by waters of the warm South Equatorial and Panama currents, and the cold Humboldt Current (Liu et al., 2014), whereas individuals from the Ecuadorian mainland coast were caught near the border with Peru, and they are heavily influenced by the Humboldt Current System, which is perhaps the most productive in terms of fish catches (Liu et al., 2007), and seasonal nutrient-enriched upwellings (Mollier-Vogel et al., 2012). The complexities of the interactions between these currents and the local conditions result in the Ecuadorian mainland coast area producing almost double the biomass/m<sup>2</sup> as the Galápagos Marine Reserve, which could cause higher  $\delta^{13}\text{C}$  and  $\delta^{15}\text{N}$  values in the Ecuadorian mainland coast. In addition, the enrichment of  $\delta^{15}\text{N}$  in yellowfin tuna collected in waters off Ecuador may be associated with high nitrogen inputs from riverine outflow and nutrient exports from agricultural lands and crops that enter the highly productive estuary of the Gulf of Guayaquil, Ecuador (Borbor-Cordova et al., 2006). Similarly, studies on waved albatross (*Phoebastria irrorata*) in the Galápagos found higher levels of  $\delta^{15}\text{N}$  when individuals had just arrived from their feeding grounds off Peru in comparison with the same individuals during the brooding period when foraging is constrained within the Galápagos Marine Reserve (Awkerman et al., 2007), which might correspond to a larger seasonal variation in the entire region.

## Carbon stable isotopes

We found lower  $\delta^{13}\text{C}$  values in Galápagos Marine Reserve tuna individuals than in those from the Ecuadorian mainland coast. Cherel and Hobson (2007) verified that  $\delta^{13}\text{C}$  at the base of the food chain should be reflected in top predators such as penguins in the Southern Ocean. Carbon baselines depend directly on many factors including primary productivity and abiotic factors (West et al., 2010). The  $\delta^{13}\text{C}$  is associated with biological and physical variables related to temperature-dependent concentrations of CO<sub>2</sub>, nutrient availability, and fractionation during the uptake of inorganic carbon in the photosynthesis of plankton, resulting in a direct relation between warmer temperatures and higher values of  $\delta^{13}\text{C}$ . Likewise, regions with high upwelling support high plankton growth rates and have higher  $\delta^{13}\text{C}$  values than those with poor upwelling systems (Magozzi et al., 2017). A recent study found that  $\delta^{13}\text{C}$  measurements in tuna muscle were closely linked to phytoplankton, which is consistent with spatially constrained movements, implying that tuna muscle  $\delta^{13}\text{C}$  could reflect the local carbon baseline (Logan et al., 2020). The differences we found in  $\delta^{13}\text{C}$  values therefore likely result from different local baselines at the Galápagos Marine Reserve and the Ecuadorian mainland coast, where different individuals were caught. A recent study suggested that the characteristic patterns of vertical movements of yellowfin tuna allow them to develop foraging strategies aimed at capturing prey from deeper areas during the day, which favors a longer association with island platforms (Páez-Rosas et al., 2020). Likewise, in the same study, acoustic tagging showed a strong loyalty of this species to the study area. The higher concentrations of  $\delta^{13}\text{C}$  in Ecuadorian mainland coast individuals could also be explained by the nutrient- and carbon-enriched mass of waters from the northernmost region of the Peruvian Coastal Upwelling (Pennington et al., 2006).

## Differences in Hg processing within yellowfin tuna populations

The Hg isotopic signatures we observed in yellowfin tuna are similar to those reported for this species from the open ocean and Hawaiian Islands in the Pacific (Blum & Bergquist, 2007; Blum et al., 2013), and in shark species from the Galápagos Marine Reserve (Maurice et al., 2021), indicating uniformity of Hg isotope values for top predators in the Pacific Ocean (Figure 3). However, we observed variation in the extent of photochemical processing between the Galápagos Marine Reserve and Ecuadorian mainland coast groups. This variation in  $\Delta^{199}\text{Hg}$  and  $\delta^{202}\text{Hg}$  fractionation, related to photochemical demethylation, in the Pacific Ocean has been explained by differences in feeding depths in previous studies (Figure 3; Blum et al., 2013; Madigan et al., 2018; Sackett et al., 2017). Although MeHg is the most bioavailable form of Hg in the open Pacific Ocean, mainly produced in the mesopelagic layer and especially in the oxygen minimum zones (Blum et al., 2013; Hammerschmidt & Bowman, 2012), higher values of  $\Delta^{199}\text{Hg}$  and  $\delta^{202}\text{Hg}$  are likely related to more photodemethylation of MeHg sources in the epipelagic and photic zones of the

oceanic environment (Blum & Bergquist, 2007; Blum et al., 2013; Madigan et al., 2018). Variation in  $\delta^{202}\text{Hg}$  was not directly correlated to  $\delta^{13}\text{C}$  and  $\delta^{15}\text{N}$  values, indicating that there are compounding factors outside foraging habits that drive  $\delta^{202}\text{Hg}$  values in fish tissues. Areas with high productivity can promote microbial demethylation, and hence it is possible that this reaction generates Hg sources with positive  $\delta^{202}\text{Hg}$  (Madigan et al., 2018). Internal cycling, such as demethylation, partitioning, or excretion can also alter  $\delta^{202}\text{Hg}$  in fish, seabirds, and mammals (Poulin et al., 2021), although it is unknown how these reactions affect the isotope values in wild yellowfin tuna populations. Thus we believe the differences between  $\Delta^{199}\text{Hg}$  in both the Galápagos Marine Reserve and Ecuadorian mainland coast relate to more intense photochemical demethylation occurring in the Galápagos Marine Reserve than in the Ecuadorian mainland coast, whereas variability associated with  $\delta^{202}\text{Hg}$  may relate to other nonphotochemically driven Hg processes.

Interestingly, we did not see strong coastal versus oceanic or offshore environment differences in the Ecuadorian mainland coast and Galápagos Marine Reserve, respectively, as previously observed in the Gulf of Mexico (Senn et al., 2010; Figure 2). Coastal fish in the Gulf of Mexico as well as in other studies with developed coastal regions (Balogh et al., 2015; Yin et al., 2016) often have much lower  $\Delta^{199}\text{Hg}$  and more variable  $\delta^{202}\text{Hg}$  than oceanic counterparts (Figure 3). This difference suggests that the coastal-oceanic/offshore separation between the Galápagos Marine Reserve and coastal Ecuador is not as pronounced as that observed in other oceanic studies or that other factors are driving Hg cycling, such as feeding differences (denoted by  $\delta^{13}\text{C}$ ) or ancillary Hg processing (denoted by  $\Delta^{199}\text{Hg}$ ). Furthermore, mathematical corrections to remove photochemical fractionation (Blum et al., 2013) indicate that the initial  $\delta^{202}\text{Hg}_{\text{COR}}$  of MeHg in both sets of tuna, prior to photochemical demethylation, is from a similar source. These results are consistent with those of studies that showed an apparent common marine source of bioavailable MeHg for most large pelagic fish in the Pacific Ocean (Besnard et al., 2021; Blum et al., 2013). Our data suggest that precipitation (i.e., atmospheric wet deposition) is the primary Hg exposure pathway for this portion of the southern Tropical Eastern Pacific Ocean food web due to the prevalence of positive  $\Delta^{200}\text{Hg}$  observed in the Galápagos Marine Reserve and Ecuadorian mainland coast populations. Motta et al. (2020) also concluded that precipitation is an important source tied to sinking particulates. Even though the tuna samples from the Galápagos Marine Reserve are from a region thought to be impacted by volcanism, no isotopic anomalies were observed in this population compared with that of the Ecuadorian mainland coast. Precipitation Hg signatures in Galápagos Marine Reserve and Ecuadorian mainland coast tuna likely originate by means of atmospheric transport, presumably from distant anthropogenic sources from the Pacific coast of South America including artisanal and small-scale gold mining in southern Ecuador (Carling et al., 2013). Emissions from human-made sources and industrialization in the Gulf of Guayaquil, for example, may explain THg concentrations on the order of 2.76 and

4.90 mg/kg dry weight observed in estuarine sediments and mangrove mussels (*Mytella strigata*), respectively (Calle et al., 2018). Comparably, Hg contamination (i.e., concentrations ranging from 1.92 to 3.63 mg/kg dry wt) in skin samples of bottlenose dolphins (*Tursiops truncatus*) from the Guayaquil Gulf was also recently reported (Alava et al., 2020).

During 2015 to 2016, a weak El Niño event was reported in the area, which caused shifts in the  $\delta^{15}\text{N}$  and  $\delta^{13}\text{C}$  baseline due to changes in nutrient regimes related to upwelling dynamics (Renedo et al., 2021; Zarn et al., 2020). When pooling the  $\Delta^{199}\text{Hg}$  and THg data for both the Galápagos Marine Reserve and Ecuadorian mainland coast, we infer the influence of foraging depth on THg exposure using  $\Delta^{199}\text{Hg}$  as a tracer (i.e.,  $\Delta^{199}\text{Hg}$  values decrease from the surface to aphotic waters; Blum et al., 2013). Thus large pelagic tuna (THg is higher as  $\Delta^{199}\text{Hg}$  increases) appear to be foraging on uppermost pelagic prey in shallow waters (i.e., exhibiting the highest  $\Delta^{199}\text{Hg}$ ) instead of on mesopelagic prey from the deepest waters. These changes could also be explained by shifts in the food chain composition or structure given the oceanographic patterns related to the Humboldt Current System dynamics during El Niño or La Niña events. Supporting this idea, a recent study with stable isotopes ( $\delta^{13}\text{C}$  and  $\delta^{15}\text{N}$ ) reported that tuna from Galápagos (including yellowfin tuna) present a pelagic foraging strategy (Páez-Rosas et al., 2020). A positive correlation between the two variables also suggests that foraging higher in the water column leads to elevated Hg concentrations within these fish despite the enhanced removal of MeHg in the water column due to photochemical demethylation. These results demonstrate that even within populations that have the same source of Hg, concentration differences can be driven by the potential ecological and biogeochemical cycling of Hg within a region. This information is crucial to understand this region of the Pacific, where little Hg data exist along with the environmental changes associated with climate change and ecological factors, which could exacerbate the expansion of the Eastern Pacific oxygen minimum zone (Kämpf & Chapman, 2016), affecting both Hg cycling and the populations of predatory fish.

## CONCLUSIONS

We did not find significant variation in THg between the Ecuadorian mainland coast and Galápagos Marine Reserve, which could be related to similar degrees of exposure to anthropogenic Hg contamination or natural sources such as volcanos, and different processes of methylation and transport related to contrasting ecological structures and circulation patterns across the Tropical Eastern Pacific Ocean. However, subtle changes related to upwellings and feeding depth could be tracked with carbon, nitrogen, and Hg isotopes and are important factors that can influence Hg concentrations in yellowfin tuna.

Scarce data on the feeding preferences, food web and diet composition, distribution, and habitat use of yellowfin tuna in the waters of Galápagos and Ecuador limited our understanding of the behavioral and foraging ecology in tandem with the

environmental exposure to and dietary routes of Hg in this species. A larger set of tuna fish muscle samples for Hg isotope analyses may better reflect or corroborate the isotopic signature of this species in the Tropical Eastern Pacific Ocean because the limited sample size we used may have precluded a more concerted isotope analysis. Assessing the cumulative impacts of regional climate change forcing (i.e., ocean warming, acidification, hypoxia in oxygen minimum zones, and changes in primary production) and fishing pressure on Hg bioaccumulation in this large pelagic fish species is an ecotoxicological research area of particular importance to pursue in the region. Our research contributes new baseline data on Hg contamination and isotopic signatures, helping us to understand the exposure, accumulation, and putative sources and thus support ecotoxicological risk assessment in tandem with Hg emissions mitigation in nations along the Tropical Eastern Pacific Ocean.

**Supporting information**—The Supporting Information is available on the Wiley Online Library at <https://doi.org/10.1002/etc.5458>.

**Acknowledgments**—We would like to thank the Galápagos National Park and Ministerio de Ambiente de Ecuador for facilitating the mobilization and research permits. Special thanks to the Plant Biotechnology Laboratory at Universidad San Francisco de Quito and to Nicolas Acosta for helping in the field. The present study would not have been possible without the interest and collaboration of the artisanal fishermen of the visited communities. We thank the Galápagos National Park Directorate and Ministry of Environment of Ecuador for facilitating the research permits. Our research was conducted with permits 010-2015-IC-FAU-DNB/MA, 015-016-IC-FAU-DNB/MA, and PNG-PC-10-16. We acknowledge the Rufford Foundation for funding this project, along with the Galápagos Science Center, Universidad San Francisco de Quito, University of North Carolina Wilmington, Ocean Pollution Research Unit at the Institute for the Oceans and Fisheries (University of British Columbia, Canada), and Harvard University (Cambridge, MA, USA). Instrumentation at the US Geological Survey (USGS) Mercury Research Laboratory was supported by the USGS Toxic Substances Hydrology Program. Special thanks to C. Lane, K. Rosov, A. Etherington, M. Marty, and A. Cooke for all their help with the analyses at University of North Carolina Wilmington.

**Conflict of Interest**—The authors declare no conflict of interest. Any use of trade, firm, or product names is for descriptive purposes only and does not imply endorsement by the US Government.

**Author Contributions Statement**—**Laia Muñoz-Abril**: Conceptualization; Data curation; Formal analysis; Funding acquisition; Investigation; Fieldwork; Methodology; Resources; Software; Project administration; Validation; Visualization; Writing—original draft and review & editing. **Carlos Valle**: Conceptualization; Formal analysis; Funding acquisition; Investigation; Methodology; Project administration; Resources;

Software; Supervision; Writing—review & editing. **Juan José Alava**: Conceptualization; Formal analysis; Funding acquisition; Investigation; Resources; Software; Validation; Visualization; Writing—review & editing. **Elsie Sunderland**: Conceptualization; Data curation; Formal analysis; Funding acquisition; Investigation; Resources; Software; Validation; Visualization; Writing—review & editing. **Steven Emslie**: Data curation; Formal analysis; Funding acquisition; Investigation; Resources; Software; Supervision; Validation; Visualization; Writing—review & editing. **Sarah E. Janssen**: Data curation; Formal analysis; Funding acquisition; Investigation; Resources; Software; Validation; Visualization; Writing—review & editing. **Francisco Rubianes-Landázuri**: Formal analysis; Funding acquisition; Investigation; Fieldwork; Resources; Software; Validation; Visualization, Writing—original draft; Writingreview & editing.

**Data Availability Statement**—All our data has been uploaded as Supporting Information.

## REFERENCES

- Alava, J. J., & Ross, P. S. (2018). Pollutants in tropical marine mammals of the Galápagos Islands, Ecuador: An ecotoxicological quest to the last Eden. *Marine mammal ecotoxicology: Impacts of multiple stressors on population health* (pp. 213–234). Academic Press. <https://doi.org/10.1016/B978-0-12-812144-3.00008-5>
- Alava, J. J., Calle, P., Tirapé, A., Biedenbach, G., Cadena, O. A., Maruya, K., Lao, W., Aguirre, W., Jiménez, P. J., Domínguez, G. A., Bossart, G. D., & Fair, P. A. (2020). Persistent organic pollutants and mercury in genetically identified inner estuary bottlenose dolphin (*Tursiops truncatus*) residents of the Guayaquil Gulf, Ecuador: Ecotoxicological science in support of pollutant management and Cetacean conservation. *Frontiers in Marine Science*, 7. <https://doi.org/10.3389/fmars.2020.00122>
- Awkerman, J. A., Hobson, K. A., & Anderson, D. J. (2007). Isotopic ( $\delta^{15}\text{N}$  and  $\delta^{13}\text{C}$ ) evidence for intersexual foraging differences and temporal variation in habitat use in waved albatrosses. *Canadian Journal of Zoology*, 85(2), 273–279. <https://doi.org/10.1139/Z06-202>
- Balogh, S. J., Tsui, M. T., Blum, J. D., Matsuyama, A., Woerndle, G. E., Yano, S., & Tada, A. (2015). Tracking the fate of mercury in the fish and bottom sediments of Minamata Bay, Japan, using stable mercury isotopes. *Environmental Science & Technology*, 49(9), 5399–5406. <https://doi.org/10.1021/acs.est.5b00631>
- Bergquist, B. A., & Blum, J. D. (2007). Mass-dependent and -independent fractionation of Hg isotopes by photoreduction in aquatic systems. *Science*, 318(5849), 417–420. <https://doi.org/10.1126/science.1148050>
- Besnard, L., Le Croizier, G., Galván-Magaña, F., Point, D., Kraffe, E., Ketchum, J., Martínez, R., & Schaal, G. (2021). Foraging depth depicts resource partitioning and contamination level in a pelagic shark assemblage: Insights from mercury stable isotopes. *Environmental Pollution*, 283, 117066. <https://doi.org/10.1016/j.envpol.2021.117066>
- Blum, J. D., & Bergquist, B. A. (2007). Reporting of variations in the natural isotopic composition of mercury. *Analytical and Bioanalytical Chemistry*, 388(2), 353–359. <https://doi.org/10.1007/s00216-007-1236-9>
- Blum, J. D., Drazen, J. C., Johnson, M. W., Popp, B. N., Motta, L. C., & Jamieson, A. J. (2020). Mercury isotopes identify near-surface marine mercury in deep-sea trench biota. *Proceedings of the National Academy of Sciences of the United States of America*, 117(47), 29292–29298. <https://doi.org/10.1073/pnas.2012773117>
- Blum, J. D., Popp, B. N., Drazen, J. C., Anela Choy, C., & Johnson, M. W. (2013). Methylmercury production below the mixed layer in the North Pacific Ocean. *Nature Geoscience*, 6(10), 879–884. <https://doi.org/10.1038/ngeo1918>
- Borbor-Cordova, M. J., Boyer, E. W., Mcdowell, W. H., & Hall, C. A. (2006). Nitrogen and phosphorus budgets for a tropical watershed impacted by agricultural land use: Guayas, Ecuador. *Biogeochemistry*, 79(1–2), 135–161. <https://doi.org/10.1007/s10533-006-9009-7>

- Bosch, A. C., O'Neill, B., Sigge, G. O., Kerwath, S. E., & Hoffman, L. C. (2016). Mercury accumulation in Yellowfin tuna (*Thunnus albacares*) with regards to muscle type, muscle position and fish size. *Food Chemistry*, 190, 351–356. <https://doi.org/10.1016/j.foodchem.2015.05.109>
- Bowman, K. L., Lamborg, C. H., & Agather, A. M. (2020). A global perspective on mercury cycling in the ocean. *Science of the Total Environment*, 710, 136166. <https://doi.org/10.1016/j.scitotenv.2019.136166>
- Calle, P., Monserrate, L., Medina, F., Calle Delgado, M., Tirapé, A., Montiel, M., Ruiz Barzola, O., Cadena, O. A., Dominguez, G. A., & Alava, J. J. (2018). Mercury assessment, macrobenthos diversity and environmental quality conditions in the Salado Estuary (Gulf of Guayaquil, Ecuador) impacted by anthropogenic influences. *Marine Pollution Bulletin*, 136, 365–373. <https://doi.org/10.1016/j.marpolbul.2018.09.018>
- Carling, G. T., Diaz, X., Ponce, M., Perez, L., Nasimba, L., Pazmino, E., Rudd, A., Merugu, S., Fernandez, D. P., Gale, B. K., & Johnson, W. P. (2013). Particulate and dissolved trace element concentrations in three southern Ecuador rivers impacted by artisanal gold mining. *Water, Air, and Soil Pollution*, 224(2), 1415. <https://doi.org/10.1007/s11270-012-1415-y>
- Chavez, F., Bertrand, A., Guevara-Carrasco, R., Soler, P., & Csirke, J. (2008). The northern Humboldt Current System: Brief history, present status and a view towards the future. *Progress in Oceanography*, 79, 95–105. <https://doi.org/10.1016/j.pocean.2008.10.012>
- Chen, C., Driscoll, C., Lambert, K., Mason, R., & Sunderland, E. (2012). *Sources to seafood: Mercury pollution in the marine environment*. Maine Sea Grant Publications.
- Chen, L., & Li, Y. (2019). A review on the distribution and cycling of mercury in the Pacific Ocean. *Bulletin of Environmental Contamination and Toxicology*, 102, 665–671. <https://doi.org/10.1007/s00128-019-02560-x>
- Cherel, Y., & Hobson, K. A. (2007). Geographical variation in carbon stable isotope signatures of marine predators: A tool to investigate their foraging areas in the Southern Ocean. *Marine Ecology Progress Series*, 329, 281–287. <https://doi.org/10.3354/meps329281>
- Cransveld, A., Amouroux, D., Tessier, E., Koutarakis, E., Ozturk, A. A., Bettoso, N., Miei, C. L., Bérail, S., Barre, J. P. G., Sturaro, N., Schnitzler, J., & Das, K. (2017). Mercury stable isotopes discriminate different populations of European seabass and trace potential Hg sources around Europe. *Environmental Science & Technology*, 51(21), 12219–12228. <https://doi.org/10.1021/acs.est.7b01307>
- Drevnick, P. E., Lamborg, C. H., & Horgan, M. J. (2015). Increase in mercury in Pacific yellowfin tuna. *Environmental Toxicology and Chemistry*, 34(4), 931–934. <https://doi.org/10.1002/etc.2883>
- Espinoza, P., Lorrain, A., Ménard, F., Cherel, Y., Tremblay-Boyer, L., Argüelles, J., Tafur, R., Bertrand, S., Tremblay, Y., Ayón, P., Munaron, J. M., Richard, P., & Bertrand, A. (2017). Trophic structure in the northern Humboldt Current System: New perspectives from stable isotope analysis. *Marine Biology*, 164(4), 86. <https://doi.org/10.1007/s00227-017-3119-8>
- Farrell, J., Pederson, T., Calvert, S., & Nielsen, B. (1995). Glacial-interglacial changes in nutrient utilization in the equatorial Pacific Ocean. *Nature*, 377, 514–517.
- Feng, C., Pedrero, Z., Gentès, S., Barre, J., Renedo, M., Tessier, E., Bérail, S., Maury-Brachet, R., Mesmer-Dudons, N., Baudrimont, M., Legeay, A., Maurice, L., Gonzalez, P., & Amouroux, D. (2015). Specific pathways of dietary methylmercury and inorganic mercury determined by mercury speciation and isotopic composition in zebrafish (*Danio rerio*). *Environmental Science & Technology*, 49(21), 12984–12993. <https://doi.org/10.1021/acs.est.5b03587>
- Franco-Fuentes, E., Andrade-Vera, S., Moity, N., Ramírez-gonz, J., Paz, S., Rubio, C., Hardisson, A., Gonz, D., & Guti, J. (2021). Metals in commercial fish in the Galapagos Marine Reserve: Contribution to food security and toxic risk assessment. *Journal of Environmental Management*, 286, 112188. <https://doi.org/10.1016/j.jenvman.2021.112188>
- Fuenzalida, R., Schneider, W., Garcés-Vargas, J., Bravo, L., & Lange, C. (2009). Vertical and horizontal extension of the oxygen minimum zone in the eastern South Pacific Ocean. *Deep-Sea Research Part II: Topical Studies in Oceanography*, 56(16), 992–1003. <https://doi.org/10.1016/j.dsr2.2008.11.001>
- Galland, G., Rogers, A., & Nickson, A. (2016). *Netting billions: A global valuation of tuna*. The PEW Charitable Trusts.
- Gilly, W. F., Beman, J. M., Litvin, S. Y., & Robison, B. H. (2013). Oceanographic and biological effects of shoaling of the oxygen minimum zone. *Annual Review of Marine Science*, 5(1), 393–420. <https://doi.org/10.1146/annurev-marine-120710-100849>
- Graham, B., Koch, P., Newsome, S., McMahon, K., & Aurióles, D. (2010). Using isoscapes to trace the movements and foraging behavior of top predators in oceanic ecosystems. In J. West, G. Bowen, T. Dawson, & K. Tu (Eds.), *Isoscapes: Understanding movement, pattern, and process on Earth through isotope mapping* (pp. 299–318). Springer. [https://doi.org/10.1007/978-90-481-3354-3\\_14](https://doi.org/10.1007/978-90-481-3354-3_14)
- Gruber, N., & Sarmiento, J. (1997). Global patterns of marine nitrogen fixation and denitrification. *Global Biogeochemical Cycles*, 11(2), 235–266.
- Hammerschmidt, C. R., & Bowman, K. L. (2012). Vertical methylmercury distribution in the subtropical North Pacific Ocean. *Marine Chemistry*, 132–133, 77–82. <https://doi.org/10.1016/j.marchem.2012.02.005>
- Houssard, P., Lorrain, A., Tremblay-Boyer, L., Allain, V., Graham, B. S., Menkes, C. E., Pethybridge, H., Couturier, L. I. E., Point, D., Leroy, B., Receveur, A., Hunt, B. P. V., Vourey, E., Bonnet, S., Rodier, M., Raimbault, P., Feunteun, E., Kuhnert, P. M., Munaron, J. M., & Letourneur, Y. (2017). Trophic position increases with thermocline depth in yellowfin and bigeye tuna across the Western and Central Pacific Ocean. *Progress in Oceanography*, 154, 49–63. <https://doi.org/10.1016/j.pocean.2017.04.008>
- Houssard, P., Point, D., Tremblay-Boyer, L., Allain, V., Pethybridge, H., Masbou, J., Ferriss, B. E., Baya, P. A., Lagane, C., Menkes, C. E., Letourneur, Y., & Lorrain, A. (2019). A model of mercury distribution in tuna from the Western and Central Pacific Ocean: Influence of physiology, ecology and environmental factors. *Environmental Science & Technology*, 53(3), 1422–1431. <https://doi.org/10.1021/acs.est.8b06058>
- Inter-Organization Programme for the Sound Management of Chemicals. (2008). *Guidance for identifying populations at risk from mercury exposure*. Issued by UNEP DTIE Chemicals Branch and WHO Department of Food Safety, Zoonoses and Foodborne Diseases.
- Janssen, S. E., Riva-Murray, K., Dewild, J. F., Ogorek, J. M., Tate, M. T., Van Metre, P. C., Krabbenhoft, D. P., & Coles, J. F. (2019). Chemical and physical controls on mercury source signatures in stream fish from the Northeastern United States. *Environmental Science & Technology*, 53(17), 10110–10119. <https://doi.org/10.1021/acs.est.9b03394>
- Kraepiel, A. M. L., Keller, K., Chin, H. B., Malcolm, E. G., & Morel, F. M. M. (2003). Sources and variations of mercury in tuna. *Environmental Science & Technology*, 37(24), 5551–5558. <https://doi.org/10.1021/es0340679>
- Kämpf, J., & Chapman, P. (2016). *Upwelling systems of the world: A scientific journey to the most productive marine ecosystems*. Springer. <https://doi.org/10.1007/978-3-319-42524-5>
- Le Croizier, G., Schaal, G., Point, D., Le Loc'h, F., Machu, E., Fall, M., Munaron, J. M., Boyé, A., Walter, P., Laë, R., & Tito De Morais, L. (2019). Stable isotope analyses revealed the influence of foraging habitat on mercury accumulation in tropical coastal marine fish. *Science of the Total Environment*, 650, 2129–2140. <https://doi.org/10.1016/j.scitotenv.2018.09.330>
- Liu, K., Quinones, R., & Atkinson, L. (2007). Carbon and nutrient fluxes in continental margins. In *Geosphere-biosphere programme; The Royal Swedish Academy of Sciences, Stockholm*. (Global Change\_The IGBP Series). Springer.
- Liu, M., Chen, L., He, Y., Mason, R. P., Shen, H., Yu, C., Zhang, Q., & Wang, X. (2018). Impacts of farmed fish consumption and food trade on methylmercury exposure in China. *Environment International*, 120, 333–344. <https://doi.org/10.1016/j.envint.2018.08.017>
- Liu, Y., Xie, L., Morrison, J., Kamykowski, D., & Sweet, W. (2014). Ocean circulation and water mass characteristics around the Galápagos archipelago simulated by a multiscale nested ocean circulation model. *International Journal of Oceanography*, 2014, 1–16. <https://doi.org/10.1155/2014/198686>
- Logan, J. M., Pethybridge, H., Lorrain, A., Somes, C. J., Allain, V., Bodin, N., Choy, C. A., Duffy, L., Goñi, N., Graham, B., Langlais, C., Ménard, F., Olson, R., & Young, J. (2020). Global patterns and inferences of tuna movements and trophodynamics from stable isotope analysis. *Deep-Sea Research Part II: Topical Studies in Oceanography*, 175, 104775. <https://doi.org/10.1016/j.dsr2.2020.104775>
- Lorrain, A., Graham, B., Popp, B., Allain, V., Olson, R., Hunt, B., Potier, M., Fry, B., Galván-magaña, F., Menkes, C. E. R., Kaehler, S., & Ménard, F. (2015). Nitrogen isotopic baselines and implications for estimating foraging habitat and trophic position of yellowfin tuna in the Indian and Pacific Oceans. *Deep-Sea Research Part II*, 113, 188–198. <https://doi.org/10.1016/j.dsr2.2014.02.003>
- Madigan, D. J., Li, M., Yin, R., Baumann, H., Snodgrass, O. E., Dewar, H., Krabbenhoft, D. P., Baumann, Z., Fisher, N. S., Balcom, P., & Sunderland, E. M. (2018). Mercury stable isotopes reveal influence of foraging depth on mercury concentrations and growth in Pacific Bluefin Tuna.

- Environmental Science & Technology*, 52(11), 6256–6264. <https://doi.org/10.1021/acs.est.7b06429>
- Magozzi, S., Yool, A., Vander Zanden, H. B., Wunder, M. B., & Trueman, C. N. (2017). Using ocean models to predict spatial and temporal variation in marine carbon isotopes. *Ecosphere*, 8(5), e01763. <https://doi.org/10.1002/ecs2.1763>
- Maurice, L., Croizier, G., Le Morales, G., Carpintero, N., Guayasamin, J. M., Sonke, J., Páez-Rosas, D., Point, D., Bustos, W., & Ochoa-Herrera, V. (2021). Concentrations and stable isotopes of mercury in sharks of the Galapagos Marine Reserve: Human health concerns and feeding patterns. *Ecotoxicology and Environmental Safety*, 215, 112122. <https://doi.org/10.1016/j.ecoenv.2021.112122>
- Mollier-Vogel, E., Ryabenko, E., Martinez, P., Wallace, D., Altabet, M. A., & Schneider, R. (2012). Nitrogen isotope gradients off Peru and Ecuador related to upwelling, productivity, nutrient uptake and oxygen deficiency. *Deep-Sea Research Part I: Oceanographic Research Papers*, 70, 14–25. <https://doi.org/10.1016/j.dsr.2012.06.003>
- Motta, L. C., Blum, J. D., Popp, B. N., Drazen, J. C., & Close, H. G. (2020). Mercury stable isotopes in flying fish as a monitor of photochemical degradation of methylmercury in the Atlantic and Pacific Oceans. *Marine Chemistry*, 223, 103790. <https://doi.org/10.1016/j.marchem.2020.103790>
- Muñoz-Abril, L., Torres, M. de L., Valle, C.A., Rubianes-Landazuri, F., Galván-Magaña, F., Canty, S., Teran, M., Brandt, M., Chaves, J., & Grewe, P. M. (2022). Lack of genetic differentiation in yellowfin tuna has conservation implications in the Eastern Pacific Ocean. *PLOS ONE*. <https://journals.plos.org/plosone/article?id=10.1371/journal.pone.0272713>
- Médiéu, A., Point, D., Receveur, A., Gauthier, O., Allain, V., Pethybridge, H., Menkes, C. E., Gillikin, D. P., Revill, A. T., Somes, C. J., Collin, J., & Lorrain, A. (2021). Stable mercury concentrations of tropical tuna in the south western Pacific ocean: An 18-year monitoring study. *Chemosphere*, 263, 128024. <https://doi.org/10.1016/j.chemosphere.2020.128024>
- Ménard, F., Lorrain, A., Potier, M., & Marsac, F. (2007). Isotopic evidence of distinct feeding ecologies and movement patterns in two migratory predators (yellowfin tuna and swordfish) of the western Indian Ocean. *Marine Biology*, 153, 141–152. <https://doi.org/10.1007/s00227-007-0789-7>
- Oschlies, A., Brandt, P., Stramma, L., & Schmidtko, S. (2018). Drivers and mechanisms of ocean deoxygenation. *Nature Geoscience*, 11(7), 467–473. <https://doi.org/10.1038/s41561-018-0152-2>
- Pauly, D., & Zeller, D. (2016). Catch reconstructions reveal that global marine fisheries catches are higher than reported and declining. *Nature Communications*, 7, 10244. <https://doi.org/10.1038/ncomms10244>
- Pennington, J. T., Mahoney, K. L., Kuwahara, V. S., Kolber, D. D., Calienes, R., & Chavez, F. P. (2006). Primary production in the eastern tropical Pacific: A review. *Progress in Oceanography*, 69, 285–317. <https://doi.org/10.1016/j.pocean.2006.03.012>
- Pethybridge, H., Choy, C. A., Logan, J. M., Allain, V., Lorrain, A., Bodin, N., Somes, C. J., Young, J., Ménard, F., Langlais, C., Duffy, L., Hobday, A. J., Kuhnert, P., Fry, B., Menkes, C., & Olson, R. J. (2018). A global meta-analysis of marine predator nitrogen stable isotopes: Relationships between trophic structure and environmental conditions. *Global Ecology and Biogeography*, 27(9), 1043–1055. <https://doi.org/10.1111/geb.12763>
- Pethybridge, H., Young, J., Kuhnert, P., & Farley, J. (2015). Using stable isotopes of albacore tuna and predictive models to characterize bio-regions and examine ecological change in the SW Pacific Ocean. *Progress in Oceanography*, 134, 293–303. <https://doi.org/10.1016/j.pocean.2015.03.001>
- Post, D., Layman, C., Arrington, A., Takimoto, G., Quattrochi, J., & Montaña, C. (2007). Getting to the fat of the matter: Models, methods and assumptions for dealing with lipids in stable isotope analyses. *Oecologia*, 152, 179–189. <https://doi.org/10.1007/s00442-006-0630-x>
- Poulin, B. A., Janssen, S. E., Rosera, T. J., Krabbenhoft, D. P., Eagles-smith, C. A., Ackerman, J. T., Stewart, A. R., Kim, E., Kim, J., & Manceau, A. (2021). Isotope fractionation from *in vivo* methylmercury detoxification in waterbirds. *ACS Earth and Space Chemistry*, 5, 990–997. <https://doi.org/10.1021/acsearthspacechem.1c00051>
- Páez-Rosas, D., Aurióles-Gamboa, D., Alava, J. J., & Palacios, D. M. (2012). Stable isotopes indicate differing foraging strategies in two sympatric oarbirds of the Galapagos Islands. *Journal of Experimental Marine Biology and Ecology*, 424–425, 44–52. <https://doi.org/10.1016/j.jembe.2012.05.001>
- Páez-Rosas, D., Galván-Magaña, F., Baque-Menoscal, J., Tripp-Valdez, A., Fischer, C., & Hearn, A. (2020). Trophic preferences of three pelagic fish inhabiting the Galapagos Marine Reserve: Ecological inferences using multiple analyses. *Environmental Biology of Fishes*, 103(6), 647–665. <https://doi.org/10.1007/s10641-020-00967-8>
- Rafter, P., & Sigman, D. (2016). Spatial distribution and temporal variation of nitrate nitrogen and oxygen isotopes in the upper equatorial Pacific Ocean. *Limnology and Oceanography*, 61, 14–31. <https://doi.org/10.1002/lno.10152>
- Renedo, M., Point, D., Sonke, J. E., Lorrain, A., Demarcq, H., Graco, M., Grados, D., Guti, D., Munaron, J. M., Pietri, A., Tremblay, Y., Bertrand, A., & Bertrand, S. L. (2021). ENSO climate forcing of the marine mercury cycle in the Peruvian upwelling zone does not affect methylmercury levels of marine avian top predators. *Environmental Science & Technology*, 55, 15754–15765.
- RStudio Team. (2020). *RStudio: Integrated development for R*. <http://www.rstudio.com/>
- Sackett, D. K., Drazen, J. C., Popp, B. N., Choy, C. A., Blum, J. D., & Johnson, M. W. (2017). Carbon, nitrogen, and mercury isotope evidence for the biogeochemical history of mercury in Hawaiian marine bottom-fish. *Environmental Science & Technology*, 51(23), 13976–13984. <https://doi.org/10.1021/acs.est.7b04893>
- Sardenne, F., Ménard, F., Degroote, M., Fouché, E., Guillou, G., Lebreton, B., Hollanda, S., & Bodin, N. (2015). Methods of lipid-normalization for multi-tissue stable isotope analyses in tropical tuna. *Rapid Communication in Mass Spectrometry*, 29, 1253–1267. <https://doi.org/10.1002/rcm.7215>
- Schaefer, K., & Fuller, D. (2022). Horizontal movements, utilization distributions, and mixing rates of yellowfin tuna (*Thunnus albacares*) tagged and released with archival tags in six discrete areas of the eastern and central Pacific Ocean. *Fisheries Oceanography*, 31, 84–107. <https://doi.org/10.1111/fog.12564>
- Schaefer, K., Fuller, D., & Aldana, G. (2014). Movements, behavior, and habitat utilization of yellowfin tuna (*Thunnus albacares*) in waters surrounding the Revillagigedo Islands Archipelago Biosphere Reserve, Mexico. *Fisheries Oceanography*, 23, 65–82.
- Scheuhammer, A., Braune, B., Chan, H. M., Frouin, H., Krey, A., Letcher, R., Loseto, L., Noël, M., Ostertag, S., Ross, P., & Wayland, M. (2015). Recent progress on our understanding of the biological effects of mercury in fish and wildlife in the Canadian Arctic. *Science of the Total Environment*, 509–510, 91–103. <https://doi.org/10.1016/j.scitotenv.2014.05.142>
- Senn, D. B., Chesney, E. J., Blum, J. D., Bank, M. S., Maage, A., & Shine, J. P. (2010). Stable isotope (N, C, Hg) study of methylmercury sources and trophic transfer in the northern Gulf of Mexico. *Environmental Science & Technology*, 44(5), 1630–1637. <https://doi.org/10.1021/es902361j>
- Teffer, A. K., Staudinger, M. D., Taylor, D. L., & Juanes, F. (2014). Trophic influences on mercury accumulation in top pelagic predators from off-shore New England waters of the northwest Atlantic Ocean. *Marine Environmental Research*, 101, 124–134. <https://doi.org/10.1007/s00244-015-0249-1>
- Tseng, C., Ang, S. J., Chen, Y. S., Shiao, J. C., Lamborg, C. H., He, X., & Reinfelder, J. R. (2021). Bluefin tuna reveal global patterns of mercury pollution and bioavailability in the world's oceans. *Proceedings of the National Academy of Sciences of the United States of America*, 118(38), 1–6. <https://doi.org/10.1073/pnas.2111205118>
- West, J., Bowen, G., Dawson, T., & Tu, K. (2010). *Isoscapes—Understanding movement, pattern, and process on Earth through isotope mapping*. Springer.
- Yin, R., Krabbenhoft, D. P., Bergquist, B. A., Zheng, W., Lepak, R. F., & Hurley, J. P. (2016). Effects of mercury and thallium concentrations on high precision determination of mercury isotopic composition by Neptune Plus multiple collector inductively coupled plasma mass spectrometry. *Journal of Analytical Atomic Spectrometry*, 31, 2060–2068. <https://doi.org/10.1039/C6JA00107F>
- Zarn, A. M., Valle, C. A., Brasso, R., Fetzner, W. D., & Emslie, S. D. (2020). Stable isotope and mercury analyses of the Galapagos Islands seabird community. *Marine Ornithology*, 48(1), 71–80.